Interaction free energy between planar walls in dense fluids: An Ornstein-Zernike approach with results for hard-sphere, Lennard-Jones, and dipolar systems

Phil Attard,* D. R. Bérard, C. P. Ursenbach, and G. N. Patey
Department of Chemistry, University of British Columbia, Vancouver, British Columbia, Canada V6T 1Z1
(Received 10 May 1991)

The interaction free energy per unit area between planar walls is given as a convolution of wall-solvent pair-correlation functions. This result, derived from the large radius limit of the macrosphere-solvent Ornstein-Zernike equations, and from the hypernetted-chain closure, provides a statistical-mechanical basis for the Derjaguin approximation, and is both generally applicable and computationally tractable. It is found that the interaction between hard walls in a hard-sphere fluid is oscillatory, and in good agreement with simulations. The van der Waals attraction emerges from asymptotic analyses of Lennard-Jones and dipolar fluids, and the full expression allows calculation of this quantity down to molecular separations. This is demonstrated by numerical results for dipolar fluids.

PACS number(s): 61.20.Gy, 82.70.Dd, 68.45.−v

I. INTRODUCTION

The Derjaguin approximation [1] relates the force between bodies with curved surfaces to the interaction free energy per unit area between planes. This is arguably one of the most useful results in colloid science, because curved surfaces comprise almost all systems whose properties are measured, whereas planar geometry is the one most accessible to theoretical calculation. White [2] has given a transparent albeit heuristic derivation of the Derjaguin approximation, and Ohshima *et al.* [3] and Glendinning and Russel [4] have given the next-order correction for charged spheres in the linearized Poisson-Boltzmann approximation.

In this paper, a statistical-mechanical analog of the Derjaguin approximation is derived from the macrosphere-solvent Ornstein-Zernike equations. Within the hypernetted-chain (HNC) approximation, we show that the force between macrospheres divided by π times their radius equals, in the large radius limit, the interaction free energy per unit area between walls. The latter is a one-dimensional Ornstein-Zernike convolution integral of wall-solvent pair-correlation functions, and as such its general application goes beyond the Derjaguin approximation.

We believe our result will prove useful for a variety of reasons, mainly connected with its statistical-mechanical basis. Since our derivation is rigorous, the regime of validity is clear, and successive corrections to the Derjaguin approximation in particular, and to the hypernetted-chain approximation more generally, may be applied. The expression makes direct contact with standard theories of the liquid state via the pair-correlation functions. Consequently, an extensive collection of procedures—analytic, asymptotic, and numeric—become applicable to the colloid system, and in this paper we shall use the expression to obtain a range of results. The pressure between hard walls in a hard-sphere fluid is obtained analytically in certain limits, and also numerically where good agreement with simulation data is found. Asymptotic analysis of the Lennard-Jones fluid shows a long-ranged inverse cubic profile near an isolated wall, and the well-known van der Waals attraction between walls. Asymptotic and numerical results for dipolar fluids between hard walls are also obtained. The latter are particularly interesting because they show explicitly the behavior of the van der Waals force in polar fluids at molecular separations, something not possible with the traditional Lifshitz or Hamaker theories.

The paper is laid out as follows. The formulation of the singlet Ornstein-Zernike equation for simple fluids in planar geometry is presented in Sec. II, and its history and numerical implementation are briefly reviewed. Section III contains the derivation of the result for interacting walls. The analysis for molecular fluids is summarized in Sec. IV. Analytic and numeric results for hard-sphere (Sec. V), Lennard-Jones (Sec. VI), and dipolar fluids (Sec. VII) are given. A brief conclusion completes the paper.

II. SINGLE WALL

We shall first derive the wall-solvent equation as the large radius limit of the macrosphere-solvent result. For an infinitely dilute spherical solute, species 0, in a simple fluid, species 1, the Ornstein-Zernike equation is [5]

$$h_{01}(r;R)=c_{01}(r;R)+\rho_1\int h_{01}(t;R)c_{11}(|\mathbf{r}-\mathbf{t}|)d\mathbf{t}$$
$$=c_{01}(r;R)+2\pi\rho_1\int_{-\infty}^{\infty}dz\int_0^{\infty}ds\, sh_{01}([(R+z)^2+s^2]^{1/2};R)c_{11}([R-r+z)^2+s^2]^{1/2}) . \quad (2.1)$$

Here ρ_1 is the solvent density, and h and c are the total and direct correlation functions. R is the hard-core radius that characterizes the solute-solvent system; it is the distance of closest approach of the centers of the solvent and the solute. If the solute and solvent have additive hard-sphere diameters d_0 and d_1, respectively, then $R=(d_0+d_1)/2$. The origin of the cylindrical coordinate system employed above is on the surface of the macrosphere with the z axis coinciding with the solute-solvent separation vector $\mathbf{r}$.

In the above we have made explicit the R dependence of the solute-solvent correlation functions in order to take the large radius limit. Provided that the solute-solvent pair potential remains bounded in this limit (such as hard sphere, or Lennard-Jones), then the solute-solvent correlation functions also remain well behaved and reduce to functions of the distance from the interface only. Hence measuring from contact $y=r-R$, we define

$$\lim_{R\to\infty} h_{01}(R+y;R)=h_{01}(y) , \tag{2.2a}$$

$$\lim_{R\to\infty} c_{01}(R+y;R)=c_{01}(y) . \tag{2.2b}$$

Further, in the same limit we must have $s \ll R$, and $z \ll R$ in Eq. (2.1) [because $c_{11}(t)\to 0$ as $t\to\infty$, and $-R<y=R-r\ll R$]. Consequently $[(R+z)^2+s^2]^{1/2} \sim R+z+O(R^{-1})$, and the limiting result is

$$h_{01}(y)=c_{01}(y) + 2\pi\rho_1\int_{-\infty}^{\infty} dz \int_0^{\infty} ds\, s h_{01}(z) \times c_{11}([(z-y)^2+s^2]^{1/2}) . \tag{2.3}$$

The technique of creating a planar wall from the infinite radius limit of a macrosphere was first employed in practical calculations by Perram and White [6]. The wall-solvent Ornstein-Zernike equation, (2.3), was derived by Henderson, Abraham, and Barker [7].

For a hard wall, one has the exact condition

$$h_{01}(y)=-1, \quad y<0 , \tag{2.4}$$

which expresses the exclusion of solvent from inside the wall. Now the z integral in Eq. (2.3) is dominated by regions $z\approx y$ [because $c_{11}(t)$ is short ranged], and hence one immediately see that

$$\lim_{y\to-\infty} c_{01}(y)=-1+2\pi\rho_1\int_{-\infty}^{\infty} dz \int_0^{\infty} ds\, s c_{11}([(z-y)^2+s^2]^{1/2}) =-1+\rho_1\hat{c}_{11}(0)=-\kappa_T^{-1} . \tag{2.5}$$

Here, $\kappa_T=1+\rho_1\hat{h}_{11}(0)=k_B T\partial\rho_1/\partial P$ (k_B is Boltzmann's constant, T is the absolute temperature, P is the pressure of the bulk solvent, and the caret denotes the Fourier transform) is the reduced isothermal compressibility of the solvent. The fact that neither $h_{01}(z)$ nor $c_{01}(z)$ decay to zero as $z\to-\infty$ means that their Fourier transforms do not exist (at least not classically; they may formally be expressed in terms of generalized functions). That is, one cannot numerically Fourier transform the wall-solvent correlation functions which appear in Eq. (2.3).

One way to evaluate Eq. (2.3) numerically is to treat the core contribution separately, as has been done previously [8,9]. That is, let

$$h_{01}(y)=c_{01}(y)+H(y)-C(y) , \tag{2.6}$$

where the core integral is

$$C(y)=2\pi\rho_1\int_{-\infty}^{0} dx \int_0^{\infty} ds\, s c_{11}([(z-y)^2+s^2]^{1/2}) . =2\pi\rho_1\int_y^{\infty} c_{11}(r)\left[1-\frac{y}{r}\right] r^2 dr, \quad y>0 . \tag{2.7}$$

The remaining convolution integral may be evaluated by Fourier transform methods, yielding

$$H(y)=2\pi\rho_1\int_0^{\infty} dz \int_0^{\infty} ds\, s h_{01}(z) \times c_{11}([(z-y)^2+s^2]^{1/2}) \tag{2.8}$$

$$\times\frac{1}{2\pi}\int_{-\infty}^{\infty}\tilde{H}(k)e^{-iky}dk . \tag{2.9}$$

Note that $H(y)\to 0$, $y\to\pm\infty$. Here one has

$$\tilde{H}(k)=\int_{-\infty}^{\infty} H(y)e^{iky}dy =\tilde{h}_{01}(k)\hat{c}_{11}(k) , \tag{2.10}$$

where

$$\tilde{h}_{01}(k)=\int_0^{\infty} h_{01}(y)e^{iky}dy \tag{2.11}$$

and

$$\hat{c}_{11}(k)=\frac{4\pi}{k}\int_0^{\infty} c_{11}(r)\sin(kr) r\, dr . \tag{2.12}$$

An alternative, perhaps more direct method is to define the function

$$C_{11}(|z-y|)\equiv\int_0^{\infty} c_{11}([(z-y)^2+s^2]^{1/2}) s\, ds , \tag{2.13}$$

and then Eq. (2.3) becomes

$$h_{01}(y)=c_{01}(y)+2\pi\rho_1\int_{-\infty}^{\infty} dz\, h_{01}(z)C_{11}(|z-y|) . \tag{2.14}$$

These one-dimensional integrals are straightforward to evaluate.

Note that a different way to avoid the difficulties associated with the nonexistence of the numerical Fourier transforms of the wall-solvent correlation functions is to define a wall of finite thickness surrounded on both sides by fluid. For the case of a fluid with finite-ranged potentials, such as a hard-sphere fluid, the results will not depend upon the thickness of the slab. However, this is not true for longer-ranged potentials, such as those that occur in Coulombic or polar fluids, and for these cases one cannot expect the results of a calculation made for a wall of finite thickness to agree with those for a semi-infinite half-space [10].

Three functions are related by the wall-solvent Ornstein-Zernike equation—$c_{11}(r)$, $h_{01}(y)$, and $c_{01}(y)$. The solvent-solvent direct correlation function $c_{11}(r)$ is a property of the bulk fluid and is independent of the wall. It may be calculated via the standard statistical-mechanical techniques for uniform fluids [5]. It is assumed known, and hence one has only to evaluate Eq. (2.7) or (2.13) once. One requires a closure approximation to relate $h_{01}(y)$ and $c_{01}(y)$, which is then to be solved by iteration in conjunction with Eq. (2.6) or (2.14). The formally exact closure equation is

$$h_{01}(y)=-1+\exp[h_{01}(y)-c_{01}(y)+d_{01}(y) -u_{01}(y)/k_BT] , \tag{2.15}$$

where $u_{01}(y)$ is the wall-solvent potential. Because the bridge function $d_{01}(y)$ remains largely intractable, one is forced to make some approximation. Perhaps the best-known approximation is the HNC

$$d_{01}(y)=0 . \tag{2.16}$$

A possible improvement upon the HNC is the reference hypernetted-chain (RHNC) closure, which uses hard-sphere bridge functions rather than neglecting them completely.

One can perhaps judge the accuracy of the HNC approximation for the wall-particle problem by its prediction for the contact density. The exact contact density of a fluid against a hard wall is related to the pressure of the bulk solvent by the contact theorem [5]

$$\rho_1[1+h_{01}(0^+)]=P/k_BT . \tag{2.17}$$

In contrast, the HNC approximation satisfies

$$\rho_1[1+h_{01}(0^+)]=\frac{\rho_1}{2}\left[1+\frac{1}{k_BT}\frac{\partial P}{\partial \rho_1}\right] , \tag{2.18}$$

in agreement with the exact expression only at low densities. This result appears to have been first obtained by Carnie *et al.* [11].

III. INTERACTING WALLS

The macrosphere-macrosphere Ornstein-Zernike equation is, in bipolar coordinates,

$$\begin{aligned} h_{00}(r;R)-c_{00}(r;R) &=\rho_1\int h_{01}(v;R)c_{01}(|\mathbf{r}-\mathbf{v}|;R)d\mathbf{v} \\ &=\frac{2\pi\rho_1}{r}\int_0^\infty d\sigma\,\sigma h_{01}(\sigma;R)\int_{|r-\sigma|}^{r+\sigma} d\tau\,\tau c_{01}(\tau;R) . \end{aligned} \tag{3.1}$$

In order to obtain flat plate results, we require the $R\to\infty$ limit. First we need to identify the dominant regions contributing to the integrals. We are interested in separations such that $-d<x=r-2R\ll R$. Define $s\equiv\sigma-R$ and $t\equiv\tau-R$, then, because both solute-solvent correlation functions are short ranged, the integral is dominated by regions such that $s\ll R$ and $t\ll R$. Changing the variables of integration, the lower limit of the τ integral becomes $|2R+x-s-R|-R=x-s$, and the upper limit may be extended to infinity. This gives

$$\begin{aligned} h_{00}(x+2R;R)-c_{00}(x+2R;R) &=\frac{2\pi\rho_1}{2R+x}\int_{-R}^\infty ds(s+R)h_{01}(s+R;R) \\ &\quad\times\int_{x-s}^\infty dt(t+R)c_{01}(t+R;R) . \end{aligned} \tag{3.2}$$

Note that the separation between the actual surfaces of the macrospheres is $x+d_1$. In the region $-d_1<x<0$, solvent is excluded from some region between the macrospheres, and this gives rise to the Asakura-Oosawa depletion attraction [12,13]. Now as $s\to-R$, $t\to\infty$ and $c_{01}(t+R;R)\approx0$. Therefore the integrals are dominated by regions $s\gg-R$ and $|t|\ll R$. Accordingly, we can now take the large radius limit to obtain

$$\begin{aligned} \lim_{R\to\infty}[h_{00}(x+2R;R)-c_{00}(x+2R;R)] &=\pi\rho_1R\int_{-\infty}^\infty ds\,h_{01}(s)\int_{x-s}^\infty dt\,c_{01}(t) . \end{aligned} \tag{3.3}$$

In view of this limiting result, we shall divide Eq. (3.2) by πR and differentiate with respect to separation in order to remove the second integral in Eq. (3.3). That is, we define a function

$$F_{00}^{\rm ex}(x;R)\equiv\frac{\partial}{\pi R\,\partial x}[h_{00}(x+2R;R)-c_{00}(x+2R;R)] . \tag{3.4}$$

Then defining

$$\lim_{R\to\infty}F_{00}^{\rm ex}(x;R)=F_{00}^{\rm ex}(x) , \tag{3.5}$$

one has

$$F_{00}^{\rm ex}(x)=-\rho_1\int_{-\infty}^\infty h_{01}(s)c_{01}(x-s)ds . \tag{3.6}$$

This is our central result.

The interpretation of Eqs. (3.4) and (3.6) is straightforward, at least within the hypernetted-chain approximation, which equates the excess potential of mean force to the negative of the series function (the excess quantity lacks the interaction potential, and the series function is the difference between the total and direct correlation functions, which equals their convolution). The quantity $F_{00}^{\rm ex}(x;R)$ is the solvent-mediated excess mean force between macrospheres whose surfaces are separated by

$x+d_1$, scaled by π times their radius, and in units of k_BT. A positive value of $F_{00}(x;R)$ corresponds to a repulsion. $F_{00}^{ex}(x)$ is the solvent-mediated excess interaction free energy per unit area between two semi-infinite half-spaces separated by $x+d_1$. A positive value of $F_{00}(x)$ means that the configuration is unstable with respect to infinite separation. The full functions contain the direct interaction potential that is lacking in the excess functions (denoted by a superscript). Note that $F_{00}(x)\to 0$, $x\to\infty$, and hence neither the bulk free energy nor the surface free energies contribute to Eq. (3.6).

Equating the right-hand side of Eq. (3.6) to the excess interaction free energy per unit area is only true within the hypernetted-chain approximation [$d_{00}(x)=0$]. One can write down the formally exact result

$$F_{00}(x)=u_{00}(x)/k_BT-d_{00}(x) -\rho_1\int_{-\infty}^{\infty}h_{01}(s)c_{01}(x-s)ds\ , \tag{3.7}$$

where $u_{00}(x)$ is the direct wall-wall potential per unit area, $d_{00}(x)$ is the wall-wall bridge function per unit area, and the wall-solvent correlation functions are presumed to be known exactly. There is an analogous formally exact version of Eq. (3.4). The bridge function may be taken from the limit of the macrosphere result

$$d_{00}(x)=\lim_{R\to\infty}\frac{\partial d_{00}(x+2R;R)}{\pi R\,\partial x}\ . \tag{3.8}$$

Alternatively, in the definition of the bridge function, one simply replaces one of the three-dimensional convolution integrals of each Yvon-Mayer diagram by a one-dimensional convolution. Note that in the solvent excluded region $-d_1<x<0$ one has the exact result $-\partial[k_BTF_{00}(x)-u_{00}(x)]/\partial x=-P$, where P is the bulk pressure. Note further that the interaction free energy per unit area for walls of infinite extent is a well-defined function, but that the total and the direct wall-wall correlation functions do not exist (their formal difference per unit area does).

The fact that Eq. (3.6) is the limiting form of Eq. (3.4) is characteristic of the Derjaguin approximation, which, in particular, equates the force between macrospheres scaled by their radius to the potential per unit area between plates [1,2]. Thus these equations are the statistical-mechanical analog of that classic approximation, and, we believe, the present work represents the first satisfactory microscopic derivation of that result. We emphasize that the Derjaguin approximation consists of equating $F_{00}(x;R)\approx F_{00}(x)$ for finite R, not just in the limit Eq. (3.5). In deriving Eq. (3.6) from the right-hand side of Eq. (3.1), we simply neglected all terms which were small compared to R. The obvious systematic correction to this is to retain terms of $O(R^{-1})$ throughout. Note that in order to be consistent this would also have to be done in the derivation of Eq. (2.3) from Eq. (2.1).

The HNC approximation consists of the identification of the right-hand sides of Eqs. (3.4) and (3.6) with the excess mean force and the excess interaction free energy, respectively. This is a good approximation when the bridge function may be neglected. A systematic correction to the HNC approach is Attard's binodal chain approximation [14]. In this approximation, the bridge function is expressed as the binary convolution of two ternary functions. For the wall-wall case one has

$$w_{00}^{(2)}(x)=\pi\rho_1^2\int_{-\infty}^{\infty}dx_3\int_{-\infty}^{\infty}dx_4\int_0^{\infty}dr_{34}r_{34}[\eta_{01}(x_3,x_4,r_{34})g_{11}(R_{34})\chi_{01}(x-x_3,x-x_4,r_{34}) -\eta_{01}^{*}(x_3,x_4,r_{34})h_{01}(x-x_3)h_{01}(x-x_4)]\ , \tag{3.9}$$

where $R_{34}^2=(x_3-x_4)^2+r_{34}^2$. For the definitions of the ternary functions, consult Refs. [14,15]. The convolution integrals that occur here and in the wall-solvent problem are best evaluated by two-dimensional Fourier (Hankel) transform techniques.

The numerical resolution of the HNC wall-wall free energy is straightforward. Equation (3.6) is a one-dimensional convolution integral that can be evaluated directly. The functions comprising the integrand are available from Eq. (2.3) and some closure approximation, Eq. (2.16), for example. Normally $c_{01}(z)$ is not evaluated for $z<0$, because one only applies the closure for positive argument. However, given $h_{01}(z)$, one can determine $c_{01}(z)$ for $z<0$ directly from Eq. (2.14), bearing in mind the limiting behavior, Eq. (2.5). Note that once the wall-solvent functions are known (see Sec. II), no further iteration is required to determine the wall-wall properties.

Equation (3.6) or (3.7) yields the interaction free energy between planes, and the net pressure can be obtained by differentiation. It is worth mentioning an alternative approach used by Lozada-Cassou [16]. This is based on the Ornstein-Zernike equation for a dumbbell-shaped molecule in a solvent, and the pressure between the two walls which comprise the solute molecule is determined from the solvent contact density. As mentioned above, if the walls are taken to be of finite thickness, the results may depend on the value chosen for that parameter (e.g., the electrical double layer [10]). Comparing this method to the present procedure, one would expect the dumbbell approach to be the more accurate, in principle (based upon diagrammatic considerations for a given closure), but practical considerations suggest difficulties in determining the pressure accurately from the contact density because of cancellations among large terms which often occur. Another method of determining the interaction between plates is based upon the inhomogeneous Ornstein-Zernike equation [17, 18]. For a given closure, it can be expected to be more accurate than either of the

singlet methods, Eq. (3.6), or that of Lozada-Cassou [16], although it is certainly much more numerically demanding. On the other hand, a great advantage of the present approach is that it can be applied to more realistic molecular models with relative ease (see below).

The interaction between macrospheres (as distinct form the interaction between planar walls considered here) has been treated by many authors using the Ornstein-Zernike equation (e.g., Refs. [13,19–22]). Our intermediate result for the macrosphere-macrosphere pair correlation functions, Eq. (3.3), has simultaneously and independently been presented by Henderson [23].

IV. MOLECULAR FLUIDS

For a molecular fluid of nonspherical particles, Eq. (2.3) becomes

$$h_{01}(y,\mathbf{\Omega}_1)=c_{01}(y,\mathbf{\Omega}_1)+\frac{\rho_1}{8\pi^2}\int h_{01}(\mathbf{s}\cdot\hat{\mathbf{z}},\mathbf{\Omega}_2)c_{11}(y\hat{\mathbf{z}}-\mathbf{s},\mathbf{\Omega}_2,\mathbf{\Omega}_1)\times d\mathbf{s}\,d\mathbf{\Omega}_2\ , \tag{4.1}$$

where we have chosen the normal to the wall to coincide with the z axis of the laboratory frame, and where $\mathbf{\Omega}$ denotes the Euler angles describing the orientation of the solvent molecule in the laboratory frame. We use the standard expansion in rotational invariants [24],

$$c_{11}(\mathbf{r}_{12},\mathbf{\Omega}_1,\mathbf{\Omega}_2)=\sum_{\substack{m,n,l\\ \mu,\nu}} c^{mnl}_{\mu\nu;11}(r_{12})\Phi^{mnl}_{\mu\nu}(\mathbf{\Omega}_1,\mathbf{\Omega}_2,\hat{\mathbf{r}}_{12})\ , \tag{4.2}$$

where the rotational invariants are

$$\Phi^{mnl}_{\mu\nu}(\mathbf{\Omega}_1,\mathbf{\Omega}_2,\hat{\mathbf{r}}_{12})=f^{mnl}\sum_{\mu',\nu',\gamma'}\begin{pmatrix} m & n & l\\ \mu' & \nu' & \gamma'\end{pmatrix}R^{m}_{\mu'\mu}(\mathbf{\Omega}_1)\times R^{n}_{\nu'\nu}(\mathbf{\Omega}_2)R^{l}_{\gamma'0}(\hat{\mathbf{r}}_{12})\ . \tag{4.3}$$

Here $\mathbf{r}_{12}=\mathbf{r}_2-\mathbf{r}_1$ is the intermolecular vector, and $\hat{\mathbf{r}}_{12}$ denotes its orientation. Also f^{mnl} is a nonzero constant, the term in large parentheses is the Wigner 3-j symbol, and $R^{m}_{\mu'\mu}(\mathbf{\Omega})$ is a Wigner generalized spherical harmonic [25]. It follows that the wall-solvent correlation functions may also be expanded

$$h_{01}(y,\mathbf{\Omega})=\sum_{n,\nu}h^{0nn}_{0\nu;01}(y)f^{0nn}\begin{pmatrix}0 & n & n\\ 0 & 0 & 0\end{pmatrix}R^{n}_{0\nu}(\mathbf{\Omega})\ , \tag{4.4}$$

and similarly for $c_{01}(y,\mathbf{\Omega})$.

It is straightforward to insert these expansions in to Eq. (4.1), to use the orthologonality property

$$\int R^{l}_{mn}(\mathbf{\Omega})^{*}R^{l'}_{m'n'}(\mathbf{\Omega})d\mathbf{\Omega}=\frac{8\pi^2}{2l+1}\delta_{l,l'}\delta_{m,m'}\delta_{n,n'}\ , \tag{4.5}$$

where $R^{l}_{mn}(\mathbf{\Omega})^{*}=(-1)^{m+n}R^{l}_{\bar{m}\bar{n}}(\mathbf{\Omega})$, $(\bar{m}=-m)$, and to equate coefficients of the Wigner generalized spherical harmonics (after accounting for the azimuthal integral). The result is

$$h^{0mm}_{0\mu;01}(y)-c^{0mm}_{0\mu;01}(y)=\sum_{n,l,\nu}F^{mnl}\frac{(-1)^{\nu}2\pi\rho_1}{2n+1}\times\int_{-\infty}^{\infty}h^{0nn}_{0\nu;01}(z)\mathcal{C}^{nml}_{\bar{\nu}\mu;11}(y-z)dz\ , \tag{4.6}$$

where

$$F^{mnl}=\frac{f^{0nn}\begin{pmatrix}0 & n & n\\ 0 & 0 & 0\end{pmatrix}f^{mnl}\begin{pmatrix}m & n & l\\ 0 & 0 & 0\end{pmatrix}}{f^{0mm}\begin{pmatrix}0 & m & m\\ 0 & 0 & 0\end{pmatrix}}\ , \tag{4.7}$$

and where we have defined

$$\mathcal{C}^{mnl}_{\mu\nu;11}(y-z)\equiv\int_0^{\infty}c^{mnl}_{\mu\nu;11}([(y-z)^2+r^2]^{1/2})\times P_l\left[\frac{y-z}{[(y-z)^2+r^2]^{1/2}}\right]r\,dr\ , \tag{4.8}$$

$P_l(\cos\theta)$ being the Legendre polynominal of order l. Note that the argument of the Legendre polynomial is simply the cosine of the polar angle $(y\hat{\mathbf{z}}-\mathbf{s})\cdot\hat{\mathbf{z}}/|y\hat{\mathbf{z}}-\mathbf{s}|$.

Now one has, for the case of molecules with a spherical hard core (assuming $f^{000}=1$),

$$h^{0mm}_{0\mu;01}(y)=-\delta_{m,0}\delta_{\mu,0}\ ,\quad y<0 \tag{4.9}$$

where the Kronecker delta appears, and hence, since the direct correlation function is short ranged,

$$\lim_{y\to-\infty}c^{0mm}_{0\mu;01}(y)=-\delta_{m,0}\delta_{\mu,0}\kappa_T^{-1}\ , \tag{4.10}$$

where

$$\kappa_T^{-1}=1-\frac{\rho_1}{(8\pi^2)^2}\int c_{11}(\mathbf{r}_{12},\mathbf{\Omega}_1,\mathbf{\Omega}_2)d\mathbf{r}_{12}d\mathbf{\Omega}_1d\mathbf{\Omega}_2 =1-4\pi\rho_1f^{000}\int_0^{\infty}c^{000}_{00;11}(r)r^2dr\ . \tag{4.11}$$

Turning now to the excess interaction free energy between walls, Eq. (3.6), for a molecular fluid one has

$$F^{ex}_{00}(x)=\frac{-\rho_1}{8\pi^2}\int_{-\infty}^{\infty}dz\int d\mathbf{\Omega}\,h_{01}(z,\mathbf{\Omega})c_{01}(x-z,\bar{\mathbf{\Omega}})\ . \tag{4.12}$$

Here, if $\mathbf{\Omega}=(\alpha,\beta,\gamma)$ is the orientation of the molecule with respect to one surface, then it is obvious that $\bar{\mathbf{\Omega}}=(-\alpha,\pi-\beta,-\gamma)$ is its orientation with respect to the other surface. One can show that

$$R^{l}_{mn}(\bar{\mathbf{\Omega}})=(-1)^{l+m}e^{2in\gamma}R^{l}_{m\bar{n}}(\mathbf{\Omega})^{*}\ , \tag{4.13}$$

and hence

$$\int R^{l}_{0n}(\mathbf{\Omega})R^{l'}_{0n'}(\bar{\mathbf{\Omega}})d\mathbf{\Omega}=\frac{8\pi^2(-1)^{l+n}}{2l+1}\delta_{l,l'}\delta_{n,n'}\ . \tag{4.14}$$

Inserting the invariant expansion (4.4) into Eq. (4.12), and using this orthogonality condition, one achieves the desired result

$$F_{00}^{\rm ex}(x)=-\rho_1\sum_{n,\nu}\left[f^{0nn}\begin{bmatrix}0 & n & n\\ 0 & 0 & 0\end{bmatrix}\right]^2\frac{(-1)^{n+\nu}}{2n+1}\times\int_{-\infty}^{\infty}h_{0\nu;01}^{0nn}(z)c_{0\nu;01}^{0nn}(x-z)dz\ . \quad (4.15)$$

This result is valid within the HNC approximation; it is a detail to formally include molecular bridge functions.

V. HARD-SPHERE FLUIDS

This section is concerned with hard-sphere fluids, specifically with the properties of such fluids near hard walls, and with the fluid-mediated interaction between walls. Throughout this section all lengths are expressed in units of the solvent diameter d_1, and hence the number density ρ_1 is in units of d_1^{-3}. The contact conventions are that the separation between solvent atoms is measured from their centers [$h_{11}(r)=-1$, $0\le r<1$], that solvent-wall contact occurs at zero [$h_{01}(x)=-1$, $x<0$], and that solvent is excluded from between the walls for separations less than zero (wall-wall contact actually occurs at $x=-1$). Before presenting numerical results for the pressure between walls, it is useful to discuss the behavior of the direct correlation function inside the wall, and then the excess free energy in the fluid-excluded region.

Consider the behavior of the wall-solvent excess potential of mean force $v_{01}^{\rm ex}(x)$ (i.e., the full potential of mean force less the pair potential) for the particular case when the atom is completely immersed in the wall, $x\le -1$. Since $v_{01}^{\rm ex}(x)$ is the work (due to rearrangement of the solvent) required to bring the atom from infinity to x, and since the solvent is not affected by further movement of the atom once it is fully inside the wall, then $v_{01}^{\rm ex}(x)$ must be constant in this region. Its value follows by noting that it is the difference in free energy of the solvent with the atom fixed at the two positions. At infinity the total free energy is the bulk Helmholtz free energy due to N atoms, less the entropy of the fixed atom, plus the surface free energy of the fluid in the vicinity of the wall. Inside the wall, the total free energy is the Helmholtz free energy of $N-1$ atoms plus the surface free energy. The surface free energies cancel, and the difference between the Helmholtz free energies is the chemical potential less the ideal gas entropy,

$$v_{01}^{\rm ex}(x)=-\mu_1^{\rm ex},\quad x\le -1\ . \quad (5.1)$$

In other words, the free energy change upon removing a fixed atom from the fluid is the excess chemical potential. This exact result is just the zero separation theorem [26,27].

Now suppose that some approximate theory satisfied Eq. (5.1), and that the excess potential of mean force in that approximation is only a function of $b_{01}(x)\equiv h_{01}(x)-c_{01}(x)$ (almost all approximate closures belong to this class). Since $h_{01}(x)=-1$, $x<0$, these assumptions lead one to conclude that $c_{01}(x)$ must be constant, and, provided that the approximation satisfies the Ornstein-Zernike equation, its value follows from Eq. (2.5),

$$c_{01}(x)=-\kappa_T^{-1}\quad x\le -1\ . \quad (5.2)$$

This result is wrong; it is obeyed by neither an exact theory nor by most approximate theories. [The notable exception is the Percus-Yevick approximation in which $c_{11}(r)=0$, $r>1$; in this case Eq. (5.2) follows directly from Eq. (2.3).] The reason that Eq. (5.2) does not hold for approximate theories is that in general they do not obey the exact result Eq. (5.1), and it does not hold for the exact $c_{01}(x)$ because the bridge function is not a function of $b_{01}(x)$.

For the case of the HNC approximation, diagrammatic analysis indicates that there is a single bridge diagram of order ρ_1^3 (the second diagram of the third row of Fig. 1 of Ref. [19], with the left root point representing the wall), which is not constant nor does it cancel with any other bridge diagram, nor with any nodal diagram with a bridge subdiagram. Hence the HNC approximation does not obey Eq. (5.1). Further, there remains a single nonconstant, noncanceled diagram of order ρ_1^3 in the HNC approximation to the direct correlation function. One has (in the region $-2\le x\le -1$)

$$c_{01}^{\rm HNC}(x)={\rm const}+\frac{4\pi^3\rho_1^3}{9}(x-2)^6\times\left[\frac{x^3}{4608}+\frac{x^2}{384}+\frac{25x}{2688}+\frac{17}{2520}\right]+O(\rho_1^4)\ . \quad (5.3)$$

This proves that Eq. (5.2) does not hold for the HNC approximation. This conclusion has been confirmed by numerical solution of the HNC closure for the hard-sphere fluid at a hard wall.

This rather lengthy discussion of the behavior of the direct correlation function inside the wall has been motivated by a recent paper by Malijevský *et al.* [28], who treated the hard-sphere fluid at a hard wall using a variety of approximate closures together with the erroneous Eq. (5.2). One could argue that Eq. (5.2) forces the approximation to obey the exact condition Eq. (5.1) (which might lead to a better performance of the approximation), and that in any case the departure from constancy is relatively small. While these arguments certainly have merit, it ought be understood that the results of such a procedure are not strictly HNC, and it may be confusing to label them as such.

Consider now the excess interaction free energy per unit area between walls. In the fluid excluded and interpenetration region $x<0$, one sees that it must be a linear function because the only effect of changing the separation is to change the volume of the bulk fluid. The exact expression is

$$k_BTF_{00}^{\rm ex}(x)=Px-2\sigma,\quad x<0 \quad (5.4)$$

where P is the pressure of the bulk fluid and σ is the surface tension (surface free energy per unit area) of the hard-sphere–fluid interface at a hard wall. The second term arises from the loss of two wall-fluid interfaces compared to the situation at infinite separation.

One can evaluate the first few Yvon-Mayer diagrams explicitly, including the first bridge diagram which is

$$\rho_1^2 d_{00}^{(2)}(x)=\begin{cases}0, & x\geq 0\\ \pi\rho_1^2 x^2(x^2-6)/12, & -1\leq x\leq 0\\ \pi\rho_1^2(8x+3)/12, & x\leq -1\ .\end{cases} \tag{5.5}$$

Using this in the diagrammatic expansion of the excess interaction free energy per unit area between hard walls in a hard-sphere fluid, one obtains

$$F_{00}^{\rm ex}(x)\sim\rho_1 x+\frac{\pi}{12}(8x+3)\rho_1^2+O(\rho_1^3),\quad x<0\ . \tag{5.6}$$

Now the virial expansion for the pressure is

$$P/k_BT\sim\rho_1+\frac{2\pi}{3}\rho_1^2+\frac{5\pi^2}{18}\rho_1^3+\cdots\ , \tag{5.7}$$

and the scaled particle theory [29] gives, for the surface tension of a hard-sphere fluid at a hard wall,

$$\sigma/k_BT=\frac{-\pi\rho_1^2}{8}\frac{(1+\pi\rho_1/6)}{(1-\pi\rho_1/6)^3}$$
$$\sim\frac{-\pi\rho_1^2}{8}+\cdots\ . \tag{5.8}$$

It is clear that these expansions inserted into the exact expression Eq. (5.4) are in agreement with Eq. (5.6) to order ρ_1^3.

The HNC closure neglects the bridge function, Eq. (5.5). Since this is not linear in the range $-1\leq x\leq 0$, one deduces that the HNC approximation for $F_{00}^{\rm ex}(x)$ will not be linear in this range, and hence will qualitatively differ from the exact functional form, Eq. (5.4). However, the HNC approximation does tend to the exact functional form in the (unphysical) region where the walls are overlapping. Suppose that to some acceptable approximation one has

$$c_{01}(x)=-\kappa_T^{-1},\quad x\leq Z<-1\ . \tag{5.9}$$

Then the range of integration in Eq. (3.6) may be split at two points, $s=x-Z$ and $s=0$, and one can easily show that

$$F_{00}^{\rm ex}(x)={\rm const}+\rho_1\kappa_T^{-1}x,\quad x\leq Z\ . \tag{5.10}$$

In other words, subject to the condition (5.9), the HNC predicts for the net pressure

$$\beta P(x)=-\rho_1\kappa_T^{-1}=-\rho_1\beta\frac{\partial P}{\partial\rho_1},\quad x\leq Z \tag{5.11}$$

where $\beta=1/k_BT$. This confirms that the HNC is exact only to first order in density. Hence the particular thermodynamic path to the pressure which proceeds from Eqs. (3.6) and (5.4) will only yield the first virial coefficient exactly. Compare this to the path which utilizes the contact theorem for the single wall, Eqs. (2.17) and (2.18), which will clearly give the first two virial coefficients exactly. Compare again with the HNC solution of a pure bulk hard-sphere fluid and the virial equation, in which route one obtains the first three virial coefficients exactly. This progressive loss of accuracy as one applies the singlet Ornstein-Zernike equation to the solute-solvent problem has been noted previously [3,19].

Figures 1 and 2 show the results of numerical HNC-type calculations for the pressure between hard walls in a hard-sphere fluid, obtained from the negative derivative of Eq. (3.6). These results were obtained using a grid spacing of 0.01 and 2^{12} mesh points. The bulk correlation functions were obtained using the standard fast Fourier transform method, and the wall-solvent functions were calculated using Eq. (2.6). The integral in Eq. (3.6) was evaluated by the trapezoidal rule, and a four-point finite difference formula was used to obtain the pressure. Some calculations were carried out using Verlet-Weis [30] bridge functions for the bulk, and Plischke-Henderson [31] or HNCP [19] for the wall-solvent bridge functions.

Figure 1 shows the region around contact for a low-density fluid ($\rho_1=0.2$). One can see that the pressure is repulsive just before the walls are brought to the fluid exclusion region. At separations less than this the walls are forced together by the pressure of the surrounding fluid. In the region $-1\leq x\leq 0$, the HNC is certainly not linear, but the inclusion of the first bridge diagram, Eq. (5.5), ameliorates this. The HNC pressure on this scale appears constant for $x<-1$, suggesting that one might take $Z=-1$ in Eqs. (5.11) and (5.9). The numbers themselves do show some small variation, again indicating that Eq. (5.2) is strictly incorrect, although it is a good approximation at this density.

Figure 2(a) compares the effects of different approximations to the bridge function at the higher density of $\rho_1=0.681$. The first point to note is the good agreement between the macrosphere (30 times the diameter of the solvent atoms) and the wall-wall results which confirms the applicability of the Derjaguin approximation $F_{00}(x;R)\approx F_{00}(x)$ for finite R. Similar agreement was obtained for ten diameter macrospheres. Second, inclusion of bridge functions changes the pure HNC results only slightly. (Note that only bulk and wall-solvent bridge functions were used; there is no direct wall-wall bridge function included in Fig. 2.) The discrepancies

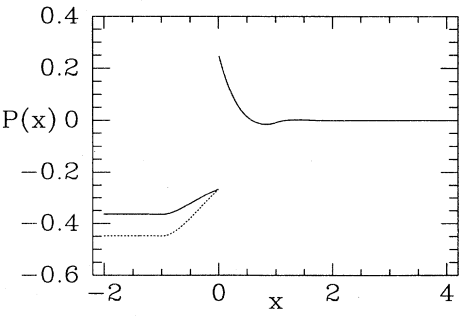

FIG. 1. Net pressure (units of $k_BTd_1^{-3}$) between hard walls in a hard-sphere fluid at a density of $\rho_1 d_1^3=0.2$ as a function of separation (units of d_1). The solid curve is the HNC result, the dotted curve is the HNC result with $d_{00}^{(2)}(x)$ given by Eq. (5.5). Note that these curves are coincident for $x>0$, and that wall-wall contact occurs at $x=-1$.

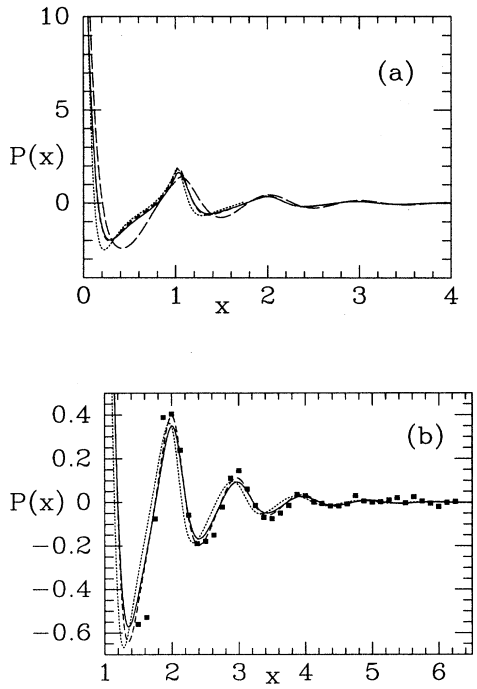

FIG. 2. Net pressure between hard walls in a hard-sphere fluid at a density of $\rho_1 d_1^3 = 0.681$ (same units as in Fig. 1). (a) The solid curve is the HNCP result for 30-diam macrospheres [19], the almost coincident dotted curve is the HNC wall-wall result, the short-dashed curve is the HNCP wall-wall result, and the long-dashed curve is the result obtained using Verlet-Weis [30] and Plischke-Henderson [31] bridge functions. (b) Comparison on an expanded scale with the simulation data of Karlström [32] (squares); the curves are the same as in (a).

caused by the use of the Plischke-Henderson [31] parametrization may be an artifact of that approximation. Third, the pressure is oscillatory in nature, with period approaching one solvent diameter, as may be expected from physical arguments.

Figure 2(b) gives a detailed comparison with the simulation data from Karlström [32]. Note that a bulk pressure of $P = 3.695 k_B T d_1^{-3}$ has been subtracted from those data in order that the net pressure approach zero at large separations. The agreement of the present theory with the simulation is quite satisfactory. (Note that a previous comparison of interacting macrospheres by two of the present authors contained plotting errors in Fig. 10 of Ref. [19] that exaggerated the discrepancy with the simulation data.) The small improvement due to the inclusion of the bridge functions in the closure cannot really be assessed because of the noise in the simulation data. In any case, the singlet HNC results are about as accurate as the inhomogeneous HNC calculations of Kjellander and Sarmen [18]. It is worth stressing that the singlet calculations are several orders of magnitude less demanding than the inhomogeneous ones. One might anticipate on the basis of these results that Eq. (3.6) will prove a fecund source of results for colloidal systems.

VI. LENNARD-JONES FLUIDS

In this section we analyze the asymptotic behavior of the solvent profile near a wall, and the interaction between walls, simple fluids with a power-law interaction potential. That is,

$$\beta u_{11}(r) \sim -Ar^{-n}, \quad n > 3, \ r \to \infty \ . \tag{6.1}$$

For the Lennard-Jones fluid, $n = 6$ and $A > 0$. The asymptotic behavior of the bulk pair correlation functions is known [14,33]

$$c_{11}(r) \sim Ar^{-n}, \quad r \to \infty \tag{6.2}$$

$$h_{11}(r) \sim \kappa_T^2 Ar^{-n}, \quad r \to \infty \ . \tag{6.3}$$

Here $\kappa_T = 1 + \rho_1 \tilde{h}_{11}(0) = [1 - \rho_1 \tilde{c}_{11}(0)]^{-1}$ is the dimensionless isothermal compressibility of the bulk solvent.

Consider now the wall-solvent Ornstein-Zernike equation (2.6). First the contribution from inside the wall, where, for large y, the solvent direct correlation function in the integrand of the first line of Eq. (2.7), may be replaced by its asymptotic form, Eq. (6.2). This gives

$$C(y) \sim \frac{2\pi\rho_1 A}{(n-2)(n-3)} y^{3-n}, \quad y \to \infty \ . \tag{6.4}$$

The integral representing the contribution from the fluid, Eq. (2.8), is dominated by two regions: $z \approx y$, in which case $h_{01}(z)$ may be replaced by $h_{01}(y)$ and brought outside the integral; and $z \approx 0$, in which case z may be neglected with respect to y in the argument of the direct correlation function. Hence

$$H(y) \sim \rho_1 \tilde{c}_{11}(0) h_{01}(y) + \frac{2\pi\Gamma_1 A}{(n-2)} y^{2-n}, \quad y \to \infty \ , \tag{6.5}$$

where $\tilde{c}_{11}(0)$ is the volume integral of the direct correlation function, and where $\Gamma_1 \equiv \rho_1 \int_{z>0} h_{01}(z) dz$ is the surface adsorption excess per unit area. The second contribution to Eq. (6.5) for the fluid side of the interface is shorter ranged by a factor of y than the contribution from within the wall, Eq. (6.4). Inserting these results into Eq. (2.6) one obtains

$$h_{01}(y) \sim \kappa_T c_{01}(y) - \frac{2\pi\rho_1\kappa_T A}{(n-2)(n-3)} y^{3-n}, \quad y \to \infty \ . \tag{6.6}$$

Now one expects that

$$c_{01}(y) \sim -\beta u_{01}(y) + O(h_{01}(y)^2) \sim By^{-m}, \quad y \to \infty \tag{6.7}$$

and so for a hard wall (or any sufficiently short-ranged wall-solvent interaction potential), only the second term will contribute in Eq. (6.6).

For the case of a Lennard-Jones fluid against a hard wall, one can see that there is a relatively long-ranged (y^{-3}) adsorption decrement. This is what one might have expected physically, since a polarizable fluid (which Lennard-Jones represents) finds an unpolarizable hard wall unfavorable. The inverse cubic tail arises from integrating the absence of r^{-6} interactions over a semi-infinite half-space. For the case of a Lennard-Jones (polarizable) wall, one would have $u_{01}(y) \sim y^{-3}$, and so the first term in Eq. (6.6) will contribute to the leading order. Whether the tail of the excess adsorption is positive or

negative depends upon the relative strengths of the Lennard-Jones parameters.

The interaction between walls may now be evaluated from Eq. (3.6). For completeness we shall include a direct wall-wall interaction potential per unit area $u_{00}(x)$ and shall assume $c_{01}(y)\sim By^{-m}$. The integral in Eq. (3.6) has three regions, which are delimited by $s=0$ and $s=x$ [note the discussion of Eq. (5.9); for the asymptotic analysis Z may be taken to be zero compared to x]. One has

$$-\rho_1\int_{-\infty}^{0} h_{01}(s)c_{01}(x-s)ds \sim \rho_1\int_{-\infty}^{0} B(x-s)^{-m}ds=\frac{\rho_1 B}{m-1}x^{1-m} \quad (6.8)$$

and

$$-\rho_1\int_{x}^{\infty} h_{01}(s)c_{01}(x-s)ds \sim \rho_1\kappa_T^{-1}\int_{x}^{\infty}\left[\kappa_T B s^{-m}-\frac{2\pi\rho_1\kappa_T A s^{3-n}}{(n-2)(n-3)}\right]ds = \frac{\rho_1 B x^{1-m}}{m-1}-\frac{2\pi\rho_1^2 A x^{4-n}}{(n-2)(n-3)(n-4)} . \quad (6.9)$$

Now in the region between the plates one has

$$-\rho_1\int_{0}^{x} h_{01}(s)c_{01}(x-s)ds \sim -\rho_1 c_{01}(x)\int_{0}^{\infty} h_{01}(s)ds-\rho_1 h_{01}(x)\int_{0}^{\infty} c_{01}(t)dt . \quad (6.10)$$

These may be neglected compared to Eqs. (6.8) and (6.9). It follows that

$$F_{00}(x)\sim\beta u_{00}(x)+\frac{2\rho_1 B}{m-1}x^{1-m}-\frac{2\pi\rho_1^2 A}{(n-2)(n-3)(n-4)}x^{4-n}, \quad x\to\infty . \quad (6.11)$$

This is an exact result. It holds even if the bridge function in Eq. (3.7) were included, because the latter is shorter ranged.

For the case of hard walls ($B=0$) or short-ranged wall-solvent potentials ($m>3$) in a Lennard-Jones fluid ($n=6$), only the last term contributes; the interaction free energy per unit area is negative and decays with the second power of separation. This is the well-known van der Waals attraction. This is also the case for Lennard-Jones walls [$\beta u_{00}(x)\sim Cx^{-2}$] across a vacuum or a fluid with short-ranged interactions. More generally, for Lennard-Jones walls in Lennard-Jones fluids, the various constants are related (in essence, $A\propto\alpha_1^2$, $B\propto\alpha_1\alpha_0$, and $C\propto\alpha_0^2$; physically the Lennard-Jones parameters depend upon atomic polarizabilities) and one can write Eq. (6.1) as a perfect square. This result, that the van der Waals force between identical half-spaces is always attractive, has long been known on the basis of Hamaker theory, and has also been shown to hold for Lifshitz theory [34].

One advantage of the asymptotic result Eq. (6.11) is that it does provide a microscopic basis for the Hamaker constant in terms of the Lennard-Jones parameters which are known for a variety of polarizable fluids and substrates. Although the asymptotic result is clearly inapplicable at small separations (where it diverges, as do Hamaker and Lifshitz theory), Eq. (3.6) is useful even up to contact. This provides for the first time a way of calculating the van der Waals force at molecular separations.

VII. DIPOLAR FLUIDS

The dipolar fluid considered here consists of hard spheres each with an embedded point dipole of moment μ. In the wall-solvent case, the lower indices of the rotational invariants vanish because of the cylindrical symmetry (see Sec. IV), which reduces them to Legendre polynomials. Further, only even terms appear in the expansion because of charge-reversal symmetry. Asymptotically, the solvent profile is [35,36]

$$h_{01}(x,\theta)\sim Ax^{-3}+BP_2(\cos\theta)x^{-3}, \quad x\to\infty \quad (7.1)$$

where θ is the angle the dipole makes with the normal to the wall. We shall require the value of the first coefficient, and this is [35, 36]

$$A=\frac{-\kappa_T}{16\pi}\frac{\epsilon-1}{\epsilon(\epsilon+1)}\left[\frac{\partial\epsilon}{\partial\rho_1}\right]_T \quad \text{(exact)} \quad (7.2a)$$

$$=\frac{-\kappa_T}{32\pi\rho_1}\left[\frac{\epsilon-1}{3y}\right]^2\left[\frac{\epsilon-1}{\epsilon}\right]^2 \quad \text{(HNC)} , \quad (7.2b)$$

where ϵ is the dielectric constant of the fluid and $y\equiv 4\pi\mu^2\rho_1/9k_BT$. Note that the dipolar fluid exhibits an inverse cubic adsorption decrement near an isolated hard wall, just as does the Lennard-Jones system. Another point of similarity is that the direct correlation function decays as the sixth power of distance from the wall. These mean that the asymptotic behavior of the excess free energy per unit area between hard walls in the dipolar fluid is determined by the same region of integration as for the Lennard-Jones, namely beyond the plate [cf. Eq. (6.9)] where the direct correlation function is constant, Eq. (4.10). The exact asymptotic result is

$$F_{00}^{\text{ex}}(x)\sim\frac{\rho_1\kappa_T^{-1}A}{2x^2}, \quad x\to\infty . \quad (7.3)$$

This is again the van der Waals attraction.

The RHNC approximation has been solved for dipolar fluids against a hard wall [36], and the results are here applied to the interacting wall problem as described in Sec. IV. In brief, the computations were performed with a grid spacing of 0.01 and 2^{12} mesh points, and four even rotational invariant projections [up to $n=6$ in Eq. (4.15)] were retained. No bridge functions were used for the wall-wall properties, but the HNCP [19] hard-sphere bridge functions were used for the wall-solvent reference; these gave a slightly smaller amplitude and a reduced period of oscillations in the pressure compared to Plischke-Henderson [31].

Figure 3(a) indicates that at smaller separations the pressure is qualitatively similar to the pure hard-sphere fluid, being oscillatory with period essentially determined by the hard-sphere diameter. The main effect of increas-

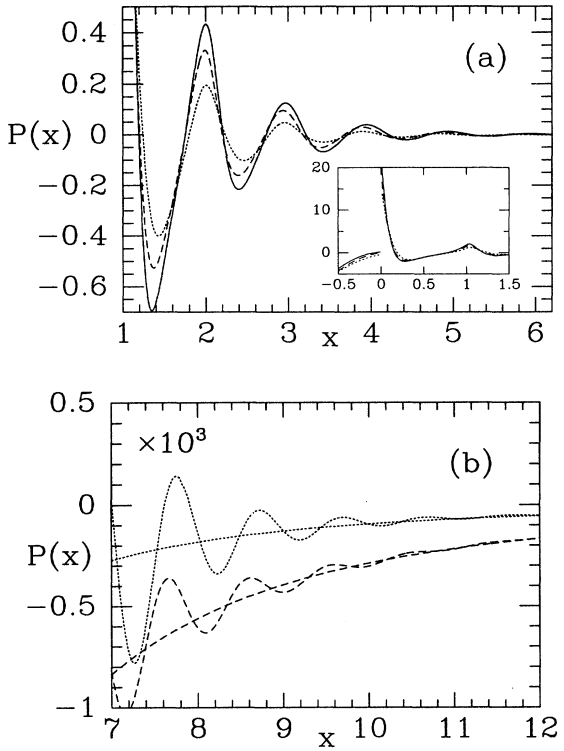

FIG. 3. HNCP pressure between walls in dipolar hard-sphere fluids at a density of $\rho_1 d_1^3 = 0.7$ (same units as in Fig. 1). (a) The solid curve is for pure hard spheres ($\mu = 0$), the dashed curve is for a reduced dipole moment of $\mu/(k_B T d_1^3)^{1/2} = \sqrt{2}$, and the dotted curve is for $\mu/(k_B T d_1^3)^{1/2} = \sqrt{3}$. (b) Magnified comparison with the HNC asymptote, Eq. (7.3), using Eq. (7.2b) (smooth curves).

ing the dipole moment is to smooth the oscillations, which could have been expected on fairly general grounds for slowly varying potentials. The inset to the figure shows that the pressure becomes highly repulsive just before fluid is completely excluded from between the walls. The asymptotic behavior of the pressure is shown in Fig. 3(b). Here there is a qualitative difference between dipolar and pure hard-sphere fluids. The latter oscillate about zero, whereas the pressure at large separations in a dipolar fluid is attractive, on average, and reasonably well described by Eq. (7.3).

These results may be contrasted with the traditional Hamaker or Lifshitz theories for the van der Waals force. In essence these correspond to extrapolating the smooth asymptotes shown in Fig. 3(b) into contact. The present theory gives a molecular prescription for calculating the Hamaker constant H. Explicitly, using Eqs. (7.2a) and (7.3), one finds that

$$H \equiv -6\pi\rho_1 k_B T \kappa_T^{-1} A = \frac{3k_B T \rho_1}{8} \frac{\epsilon - 1}{\epsilon(\epsilon+1)} \left[\frac{\partial \epsilon}{\partial \rho_1} \right]_T = \frac{3(k_B T)^2}{8\rho_1 \kappa_T} \frac{\epsilon - 1}{\epsilon + 1} \left[\frac{\partial \ln \epsilon}{\partial P} \right]_T . \quad (7.4)$$

Here we have used Eq. (55) of Ref. [37] to obtain the final convenient form. This expression for the Hamaker constant is exact for solvents modeled as rigid dipolar particles and contained between inert walls. For water, the measured logarithmic pressure derivative of the dielectric constant and the isothermal compressibility are tabulated [38,39]. Using these, we obtain $H = 1.56 \times 10^{-21}$ J as the Hamaker constant for water between inert walls at 25 °C. For the dipolar fluid of Fig. 3 with the reduced dipole moment of $\sqrt{3}$ ($\epsilon = 49.2$), the Hamaker constant from Eq. (7.4) is $H = 6.99 \times 10^{-21}$ J, which is about 4 times smaller than predicted by the HNC approximation, Eq. (7.2b). These values are comparable to those often used for hydrocarbon-water systems [40].

Besides providing a microscopic basis for the Hamaker constant, which may be used to estimate the long-range part of the van der Waals force, the present theory also correctly takes into account molecular size, predicting that the pressure is oscillatory, for example. A further important achievement is that the theory properly describes the behavior near contact. The traditional theories predict a monotonic attraction which diverges at contact (adhesion), whereas these results show that there is a very steep repulsion before wall-wall contact is attained, and that in fact the surfaces are likely to sit in one of the minima in the free energy, separated by several solvent diameters.

VIII. CONCLUSION

The wall-wall Ornstein-Zernike equation derived in this paper should prove useful because it allows the interaction free energy between planes—a quantity of importance both conceptually and practically—to be readily calculated using the standard techniques of statistical mechanics. Further, the rigorous microscopic derivation of the Derjaguin approximation also given here will enable theoretical results for walls to be applied to experiments on curved surfaces with some confidence. If necessary, both the Derjaguin and HNC approximations can be systematically corrected, as was discussed in the text.

The pressure between hard walls in a hard-sphere fluid was found to be oscillatory, with the period slightly greater than the hard-sphere diameter. Good agreement with simulation data was observed, and the HNC results were only marginally changed by inclusion of the wall-solvent bridge function. Of academic interest is the fluid excluded region, and here a detailed analysis of the error in the HNC was given. It was demonstrated that this particular route to the bulk pressure would yield only the first virial coefficient.

Asymptotic analysis of the Lennard-Jones fluid revealed a long-ranged (inverse cubic) desorption near an isolated hard wall, and an attractive interaction free energy decaying with the second power of separation between two identical half-spaces. The latter was discussed in terms of the well-known van der Waals attraction, and hence a quantitative microscopic basis for the Hamaker constant in terms of Lennard-Jones parameters is now available. The full result will enable the calculation of the van de Waals force between surfaces in polarizable

fluids down to molecular separations, an unresolved problem in the traditional Hamaker or Lifshitz theories which are really asymptotic in nature.

Results for dipolar hard spheres between hard walls were also given. It was found that the dipole moment smoothed the oscillatory pressure compared to the pure hard-sphere result. At larger separations the attractive net pressure decayed as an inverse cubic—the van de Waals attraction for a polar fluid. These represent the first theoretical results for the interaction between walls in a molecular fluid. This may become the major application of the present theory, since there appears no comparable alternative for describing the forces between surfaces across fluids composed of nonspherical molecules.

ACKNOWLEDGMENTS

The financial support of the Natural Sciences and Engineering Research Council of Canada, and of the Network of Centres of Excellence Programme in association with the Natural Sciences and Engineering Research Council of Canada, is gratefully acknowledged. One of us (P.A.) thanks the Killam Foundation of the University of British Columbia for financial support.

*Present address: Department of Applied Mathematics, Research School of Physical Sciences, Australian National University, Canberra, Australian Capital Territory 2601, Australia.

[1] B. V. Derjaguin, Kolloid Z. **69**, 155 (1934).
[2] L. R. White, J. Colloid Interface Sci. **95**, 286 (1983).
[3] H. Ohshima, D. Y. C. Chan, T. W. Healy, and L. R. White, J. Colloid Interface Sci. **90**, 17 (1982).
[4] A. B. Glenndinning and W. B. Russel, J. Colloid Interface Sci. **93**, 95 (1983).
[5] J. P. Hansen and I. R. McDonald, *Theory of Simple Liquids* (Academic, New York, 1976).
[6] J. W. Perram and L. R. White, Discuss. Faraday Soc. **59**, 29 (1975).
[7] D. Henderson, F. F. Abraham, and J. A. Barker, Mol. Phys. **31**, 1291 (1976).
[8] D. E. Sullivan and G. Stell, J. Chem. Phys. **69**, 5450 (1978).
[9] G. M. Torrie, J. P. Valleau, and G. N. Patey, J. Chem. Phys. **76**, 4615 (1982).
[10] M. Lozada-Cassou and E. Díaz-Herrera, J. Chem. Phys. **92**, 1194 (1990).
[11] S. L. Carnie, D. Y. C. Chan, D. J. Mitchell, and B. W. Ninham, J. Chem. Phys. **74**, 1472 (1981).
[12] S. Asakura and F. Oosawa, J. Chem. Phys. **22**, 1255 (1958).
[13] P. Attard, J. Chem. Phys. **91**, 3083 (1989).
[14] P. Attard, J. Chem. Phys. **93**, 7301 (1990); **94**, 6936 (E) (1991).
[15] P. Attard, J. Chem. Phys. **95**, 4471 (1991).
[16] M. Lozada-Cassou, J. Chem. Phys. **80**, 3344 (1984).
[17] R. Kjellander and S. Marčelja, J. Chem. Phys. **82**, 2122 (1985).
[18] R. Kjellander and S. Sarmen, Chem. Phys. Lett. **149**, 102 (1988).
[19] P. Attard and G. N. Patey, J. Chem. Phys. **92**, 4970 (1990).
[20] G. N. Patey, J. Chem. Phys. **72**, 5763 (1980).
[21] L. Belloni, Chem. Phys. **99**, 43 (1985).
[22] D. Henderson and M. Lozada-Cassou, J. Colloid Interface Sci. **114**, 180 (1986).
[23] D. Henderson, Proceedings of the Eleventh Symposium of Thermophysical Properties, Boulder, 1991 [Fluid Phase Equilibria (to be published)].
[24] L. Blum and A. J. Torruella, J. Chem. Phys. **56**, 303 (1972); L. Blum, *ibid.* **57**, 1862 (1972); **58**, 3295 (1973).
[25] A. Messiah, *Quantum Mechanics* (Wiley, New York, 1962), Vol. II.
[26] W. G. Hoover and J. C. Poirer, J. Chem. Phys. **37**, 1041 (1962).
[27] E. Meeron and A. J. F. Siegert, J. Chem. Phys. **48**, 3139 (1968).
[28] A. Malijevský, R. Pospíšil, W. R. Smith, and S. Labík, Mol. Phys. **72**, 199 (1991).
[29] H. Reiss, H. L. Frisch, and J. L. Lebowitz, J. Chem. Phys. **31**, 369 (1959).
[30] L. Verlet and J. J. Weiss, Phys. Rev. A **5**, 939 (1972).
[31] D. Henderson and M. Plischke, Proc. R. Soc. London Ser. A **400**, 163 (1985).
[32] G. Karlström, Chem. Scr. **25**, 89 (1985).
[33] G. Stell, *Statistical Mechanics. Part A: Equilibrium Techniques,* edited by B. J. Berne (Plenum, New York, 1977).
[34] P. Attard and D. J. Mitchell, J. Chem. Phys. **88**, 4391 (1988).
[35] J. P. Badiali, J. Chem. Phys. **90**, 4401 (1989).
[36] D. R. Bérard and G. N. Patey, J. Chem. Phys. **95**, 5281 (1991).
[37] P. G. Kusalik and G. N. Patey, J. Chem. Phys. **86**, 5110 (1986).
[38] B. B. Owen, R. C. Miller, C. E. Milner, and H. L. Cogan, J. Phys. Chem. **65**, 2065 (1961).
[39] *CRC Handbook of Chemistry and Physics,* 66th ed., edited by R. C. Weast (Chemical Rubber, Cleveland, 1985).
[40] J. Mahanty and B. W. Ninham, *Dispersion Forces* (Academic, London, 1976).